GEOPHYSICAL RESEARCH LETTERS, VOL. 26, NO. 23, PAGES 3493-3496, DECEMBER 1, 1999

Steady-state flow of solid CO_2: Preliminary results

William B. Durham

University of California Lawrence Livermore National Laboratory, Livermore, CA 94550

Stephen H. Kirby and Laura A. Stern

U. S. Geological Survey, MS 977, 345 Middlefield Rd, Menlo Park CA 94025

Abstract. To help answer the question of how much solid CO_2 exists in the Martian south polar cap, we performed a series of laboratory triaxial deformation experiments at constant displacement rate in compression on jacketed cylinders of pure, polycrystalline CO_2. Test conditions were temperatures $150 < T < 190$ K, hydrostatic confining pressures $5 \le P \le 40$ MPa, and strain rates $4.5 \times 10^{-8} \le \dot{\varepsilon} \le 4.3 \times 10^{-4}$ s^{-1}. Most of the measurements follow a constitutive law of the form $\dot{\varepsilon} = A\sigma^n \exp(-Q/RT)$, where σ is the applied differential stress, R is the gas constant, and the other constants have values as follows: $A = 10^{3.86}$ $MPa^{-n}s^{-1}$, $n = 5.6$, and $Q = 33$ kJ/mol. Solid CO_2 is markedly weaker than water ice. Our results suggest that the south polar cap on Mars is unlikely to be predominately solid CO_2, because the elevation and estimated age of the cap is difficult to reconcile with the very weak rheology of the material.

1. Introduction

Water is the principal component of the residual ice caps at the Martian poles [see review by *Thomas et al.*, 1992]. A CO_2 seasonal cap forms at the poles, but in the north polar region, summer temperatures are too warm to allow any CO_2 to survive in the residual cap. However, CO_2 frost does persist year round at the south polar cap [*Keiffer*, 1979; *Paige and Keegan*, 1994], and hence CO_2 could possibly exist at depth as an important component.

Clark and Mullin [1976] noted morphological evidence for "glacial" movements in the Mariner 9 images of the polar caps. Since Martian surface temperatures are far too low to allow water ice to flow at significant rates under ice cap stresses, Clark and Mullin searched for an explanation in CO_2 flow, and carried out the first experiments on the strength of solid CO_2 in the laboratory. They found CO_2 to be profoundly weaker than ice, and using a simple Orowan model [*Clark and Mullin*, 1976] for the gravitational spreading of an ice cap with a parabolic profile, found that a CO_2 ice cap could indeed spread rapidly enough at Martian temperatures to produce distinct flow features.

The *Clark and Mullin* [1976] experiments had two shortcomings. The first was an experimental difficulty with temperature control, restricting the duration of the experiments and thus the range of strain rates that could be explored. The second and more serious problem involved leaky pressure seals, which forced them to run at 1-atm pressure. They acknowledged the possibility that lack of confinement might not suppress brittle deformation, but they argued that smooth stress-strain curves and the lack of visible microfractures at 40 × optical examination indicated no obvious departure of the imposed deformation from pure ductility.

We conducted a suite of triaxial experiments using jacketed samples so that the confining pressure was independent of pore pressure. We confirm the basic finding of Clark and Mullin that CO_2 is far weaker than water ice, but we document somewhat higher strengths and different flow law parameters than those indicated by their earlier unconfined tests. In a separate paper [*Nye et al.*, 2000] we apply our findings to the question of the gravitational stability of a putative CO_2 south polar cap on Mars and reach the conclusion that the cap is unlikely to be composed only of CO_2.

2. Experimental Techniques and Results

Polycrystalline samples of fully dense, solid CO_2 were made in the laboratory by disaggregating blocks of standard-grade dry ice with hammer blows and then hot pressing cylinders 25 mm in diameter and 63 mm long. The disaggregated material had the texture of a uniform sand, and we estimate the grain diameter to be within a factor of two of 0.25 mm. We hot pressed by hand using a table-top press and a chilled die that steadily warmed in room air. Good densification was evident in the conversion of the compact from an opaque white to a waxy gray appearance and probably occurred at temperatures within a few degrees of 195 K, the 1-atm sublimation temperature for solid CO_2. We did not quantify grain size or hot pressing temperature further, but made every attempt to use identical preparation techniques for every sample. Some of the preparation steps were performed in room air, but sublimating samples after experimentation produced less than 0.1 wt.% H_2O in the test material.

Experiments were carried out in a cryogenic triaxial gas apparatus designed specifically for testing planetary ices at low stresses and strain rates [*Heard et al.*, 1990]. Cylindrical samples (Figure 1) were deformed in triaxial compression by shortening at fixed rates while under confining pressures of 5 and 10 MPa. One measurement was made at 40 MPa. CO_2 pressure in the sample was fixed at 1 atm. The measured variable was differential stress (σ). By testing at different temperatures (T) and strain rates ($\dot{\varepsilon}$) one can determine the parameters of the conventional creep equation

$$\dot{\varepsilon} = A\sigma^n \exp(-Q/RT) \qquad (1)$$

where R is the gas constant, and A, n, and Q are material constants. To seal the samples against confining pressure, we encapsulated them in soft, thin-walled (0.25 mm) In tubes. Reported strengths are corrected for jacket strength, based on our own calibration measurements on pure In at these same conditions.

Measurements were made in the "apparent" steady-state regime, usually achieved after a few percent strain at a given strain rate, where σ and $\dot{\varepsilon}$ become independent of strain and time. We use the qualifier "apparent" in the absence of

Paper number 1999GL008373.
0094-8276/99/1999GL008373$05.00

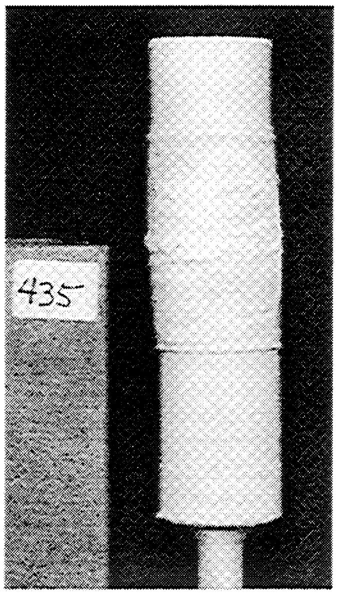

Figure 1. Polycrystalline CO_2 sample 435 after testing, still sealed in its In jacket and attached (at the bottom) to the internal force gauge. Diameter of end plug at the top is 26 mm. The near cylindrical shape is typical and indicates that strain was approximately uniform throughout testing.

detailed observations that confirm that the microstructural state of the material does not continue to evolve with strain. Five samples of hot-pressed CO_2 were tested at conditions of $150 < T < 190$ K, $4.5 \times 10^{-8} \leq \dot{\varepsilon} \leq 4.3 \times 10^{-4}$ s^{-1}, and $5 \leq P \leq 40$ MPa (Table 1). The runs were multiple-step; when steady state was achieved in a given step, the displacement rate was changed to a new fixed level, and stress was again followed to its new steady-state level.

The results for all steady-state stress measurements are shown in Figure 2. The lines in the figure correspond to the flow law (1) with $A = 10^{3.86}$ $MPa^{-n}s^{-1}$, $n = 5.6$ and $Q = 33$ kJ/mol. This fit minimizes the number of data points (there are 6) for which the fit falls outside the estimated errors in σ and T. A conventional least-squares fit of all the data points, ignoring the varying sizes of the error bars, gives $A = 10^{3.60}$ $MPa^{-n}s^{-1}$, $n = 5.2$, and $Q = 31.6$ kJ/mol with a correlation coefficient of 0.95.

3. Analysis and Discussion

We compare on normalized coordinates in Figure 3 the strength results with those measured in the same apparatus for water ice [*Durham et al.*, 1997] and to the earlier measurements of *Clark and Mullin* [1976]. Accounting for the higher melting temperature (T_m) and shear modulus (μ) for H_2O, it can be seen that CO_2 is profoundly weaker than water ice – by a factor of well over 10 at the conditions tested. There is little chance of confusing H_2O and CO_2 on a rheological basis on the surface of Mars. Clark and Mullin found CO_2 to be slightly weaker than we did, plausibly the result of the activation of one or more volume-dependent deformation mechanisms in the Clark and Mullin tests, which were suppressed in our tests by confining pressure. Microfracturing seems an unlikely explanation, since the data sets converge at lower temperature and higher strain rates where microfracturing should be more pronounced. Besides the overall low strength, the most remarkable feature of the rheology of CO_2 is an unusually strong sensitivity of strain rate to stress, which may have escaped notice by Clark and Mullin because of their narrow range of strain rate. The high stress sensitivity, characterized by a stress exponent of 5 to 7 or more, persists to the lowest stresses we are able to apply.

Also plotted in Figure 3 are strength measurements for solid methane, the only other van der Waals bonded material for which meaningful strength data exist, from a compilation by *Eluszkiewicz and Stevenson* [1990]. At comparable homologous temperatures T/T_m, solid CH_4 is about one-half order of magnitude weaker (in σ/μ) than CO_2. *Yamashita and Kato* [1997] performed rough penetrator and stress relaxation experiments on both CH_4 and CO_2. Based on a pair of measurements at $T_m/T \approx 1.1$ they found CH_4 to be weaker than CO_2 by roughly one order of magnitude.

One exploratory measurement at $P = 40$ MPa (Table 1) vs. all others at 5 and 10 MPa shows that confining pressure does not have a first-order influence on strength. The small pressure effect confirms that all results here apply to the ductile field and that for the near-surface environment of the planets, at least, pressure is not an important variable where ductile flow is concerned.

The uncertainties evident in Figure 2 are larger than is typical for other icy materials tested in this apparatus, so are a matter of some concern. If we examine the data on a run by run basis (Figure 4), it becomes quite clear that much of the scatter in Figure 2 is sample-to-sample variability, even while individually the runs produce self-consistent and very reproducible strength data. For example, direct strain-rate stepping in runs 433 (Figure 4b) and 435 (Figure 4c) independently indicated $n = 7 \pm 2$ (range allowed by error bars

Table 1. Run Data

Run (step)	P, MPa	T, K	strain	strain rate $\dot{\varepsilon}$, s^{-1}	stress σ, MPa
427(4)	10	174.0 ± 2.0	0.155	3.92×10^{-5}	2.1 ± 0.20
427(6)	10	184.0 ± 2.0	0.190	4.10×10^{-5}	1.3 ± 0.30
433(1)	10	175.0 ± 1.5	0.045	3.56×10^{-6}	1.6 ± 0.20
433(3)	10	175.0 ± 1.5	0.124	3.88×10^{-4}	3.1 ± 0.30
433(5)	10	159.5 ± 2.0	0.149	4.00×10^{-6}	2.4 ± 0.20
433(7)	10	159.5 ± 2.0	0.207	4.29×10^{-4}	4.7 ± 0.30
435(1)	5	185.5 ± 1.5	0.049	3.58×10^{-7}	0.80 ± 0.15
435(2)	5	185.5 ± 1.5	0.110	3.83×10^{-6}	0.95 ± 0.10
435(4)	5	186.0 ± 2.0	0.131	3.92×10^{-7}	0.75 ± 0.10
435(6)	5	185.5 ± 1.5	0.189	4.20×10^{-5}	1.3 ± 0.15
435(8)	5	185.5 ± 2.0	0.217	4.35×10^{-7}	0.70 ± 0.15
438(1)	5	189.0 ± 1.5	0.048	3.72×10^{-5}	1.5 ± 0.20
438(2)	5	179.0 ± 2.0	0.103	3.95×10^{-5}	1.8 ± 0.15
438(3)	5	164.0 ± 3.0	0.153	4.19×10^{-5}	2.2 ± 0.25
438(4)	5	152.0 ± 1.5	0.193	4.39×10^{-5}	2.8 ± 0.25
438(5)	5	188.5 ± 2.0	0.239	4.66×10^{-5}	1.3 ± 0.15
[1]438a(7)	40	173.0 ± 2.5	0.320	5.22×10^{-5}	2.0 ± 0.20
438a(8)	5	173.0 ± 2.5	0.356	5.53×10^{-5}	1.8 ± 0.20
440(1)	5	190.5 ± 1.5	0.052	3.49×10^{-6}	0.65 ± 0.10
440(3)	5	175.0 ± 1.5	0.091	3.65×10^{-6}	1.0 ± 0.10
440(4)	5	162.0 ± 1.5	0.129	3.80×10^{-6}	1.7 ± 0.15
440(5)	5	190.0 ± 1.5	0.163	3.96×10^{-6}	0.65 ± 0.10
[1]440a(6)	5	186.0 ± 2.0	0.192	4.10×10^{-7}	0.75 ± 0.10
440a(7)	5	171.5 ± 2.0	0.222	4.26×10^{-7}	0.80 ± 0.15
440a(8)	5	157.0 ± 2.0	0.257	4.46×10^{-7}	1.3 ± 0.15
440a(9)	5	174.0 ± 2.0	0.259	4.47×10^{-8}	0.60 ± 0.15

[1] Sample assembly removed for direct observation of shape, then returned to apparatus without rejacketing; run number appended with letter "a."

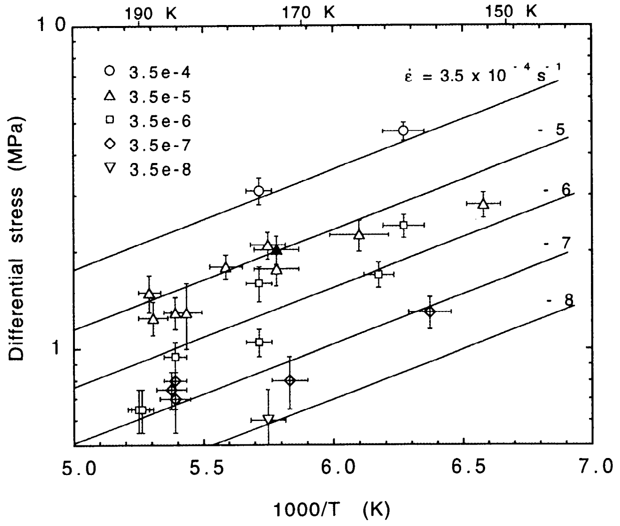

Figure 2. Steady-state flow data for solid CO_2. Lines show an estimated fit to the data for the case of equal weighting of all points (see text) at five different strain rates, each separated by one order of magnitude. Open symbols represent data at a confining pressure P of 5 or 10 MPa; the one closed symbol (a triangle) represents an experiment at $P = 40$ MPa.

in Figures 4b and c), although the overall rheologies of those two runs are not consistent with a single law. Direct temperature stepping at fixed strain rate constrains the ratio Q/n. The overall fit in Figure 2 corresponds to $Q/n = 5.9$ kJ/mol. Run 438 (Figure 4d) yields $Q/n = 4.6 \pm 0.8$ kJ/mol over a wide temperature range $152 \le T \le 189$ K, run 440 (Figure 4e) yields $Q/n = 8.7 \pm 1.1$ kJ/mol over a narrower range $162 \le T \le 190$ K, and run 427 (Figure 4a) allows a very wide range of Q/n. Note that not all the inconsistency is explainable as sample-to-sample variability: the maximum value of Q/n allowed by run 440a (Figure 4f) is about 6 kJ/mol, so data from runs 440 and 440a, two different runs on the same sample, are not even consistent with a single flow law.

The outward appearances of the samples give no obvious hint of the cause of the variation. Paradoxically, the final shapes and outer jacket textures of the samples following the six runs are typically better — both in terms of the uniformity of strain that they indicate and in terms of their sample-to-sample similarity — than is typical for other icy materials tested in this apparatus. Figure 1 (run 435) was not selected as exemplary, but truly is representative of all the runs. At this point there are simply insufficient data to understand the cause of the variability. It seems unlikely based on a long history of experiments on icy materials in this apparatus that instrumentation is at fault, and the uneventful and routine sample preparation steps do not point to any obvious cause for material variability. There may be subtleties in the preparation and handling of the material, for instance rapid grain growth under certain conditions, that we don't yet appreciate. The fact that five well-behaved runs leave us with such uncertainty suggests that further refinement of the flow law for solid CO_2 will require not a few, but many more experiments.

At this point, our most concise quantification of the rheology of solid CO_2 is as follows: (a) The recommended rheology is Equation (1) with values $A = 10^{3.86}$ $\mathrm{MPa}^{-n}\mathrm{s}^{-1}$, $n = 5.6$, and $Q/n = 5.9$ kJ/mol (i.e., the lines in Figure 2). Q/n is probably not lower than 4 nor higher than 9 kJ/mol; (b) $n = 7$ is a plausible best estimate. Constraining n to be 7, Q/n to be the same as in a), and the rheology to match the line of $\dot{\varepsilon} = 3.5 \times 10^{-6}$ s^{-1} in Figure 2, the best estimate for the flow parameters becomes $A = 10^{5.07}$ $\mathrm{MPa}^{-n}\mathrm{s}^{-1}$, $n = 7$, and $Q = 41$ kJ/mol.

In either case (a) or (b), the value of n is high compared with that for most other crystalline solids deformed at low stresses at a substantial fraction of the melting temperature. (A notable mineral group with high n are the carbonates, with $n = 7$-8 [*Heard*, 1976]). It is notable that at stresses above 1 MPa ($\sigma/\mu > 0.0005$) the van der Waals bonded CH_4 also may show a very high n (Figure 4).

The extrapolation of laboratory-derived flow laws to much lower-stress geological settings should always be done with the caveat that weaker deformation mechanisms may intervene. The warning is especially appropriate if the lab mechanism is of high n. The flow of crystalline solids is generally effected through the combined action of simultaneously operating deformation mechanisms of the form (1), so mechanisms of lower n will necessarily contribute proportionally more to total strain rate as stress decreases. As a result, mechanisms of deformation of earth materials *in situ* can be different from those observed in the laboratory [e.g., *Paterson*, 1990; *Evans and Kohlstedt*, 1995]. The $n = 5$-7 law described above should therefore be regarded as an upper bound on the strength of solid CO_2.

4. Conclusion

Conducting deformation experiments under confining pressures well in excess of the applied differential stress assures that the material is deforming in a strictly ductile

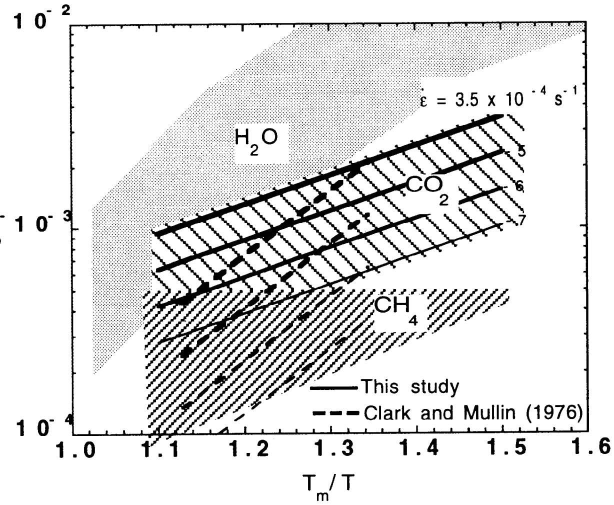

Figure 3. Flow of ices compared. Stress is normalized by shear modulus (μ) and temperature normalized by melting temperature (T_m) to facilitate comparison. Data for CO_2 ice from this study (solid lines) and that of *Clark and Mullin* [1976] (dashed lines) are shown at four values of strain rate $\dot{\varepsilon}$ as in Figure 2 (3.5×10^{-8} s^{-1} not shown), with line thickness here corresponding to strain rate. Shaded and hatched areas enclose a region bounded at top and bottom by $\dot{\varepsilon} = 3.5 \times 10^{-4}$ and 3.5×10^{-7} s^{-1}, respectively, for H_2O ice and for two van der Waals bonded ices, CO_2 and CH_4. The upper $\dot{\varepsilon}$ bound for CH_4 is horizontal to show that the deformation mechanism changes from $n = 3$ to very high n above $\sigma = 1$ MPa. Flow law for CH_4 taken from compilation by *Eluszkiewicz and Stevenson* [1990]. Constants used are T_m: H_2O (273 K), CO_2 (217 K), CH_4 (90.7 K), all values appropriate for zero pressure; μ: H_2O (3.5 GPa), CO_2 (2 GPa), CH_4 (2 GPa). The temperature sensitivity of μ is ignored.

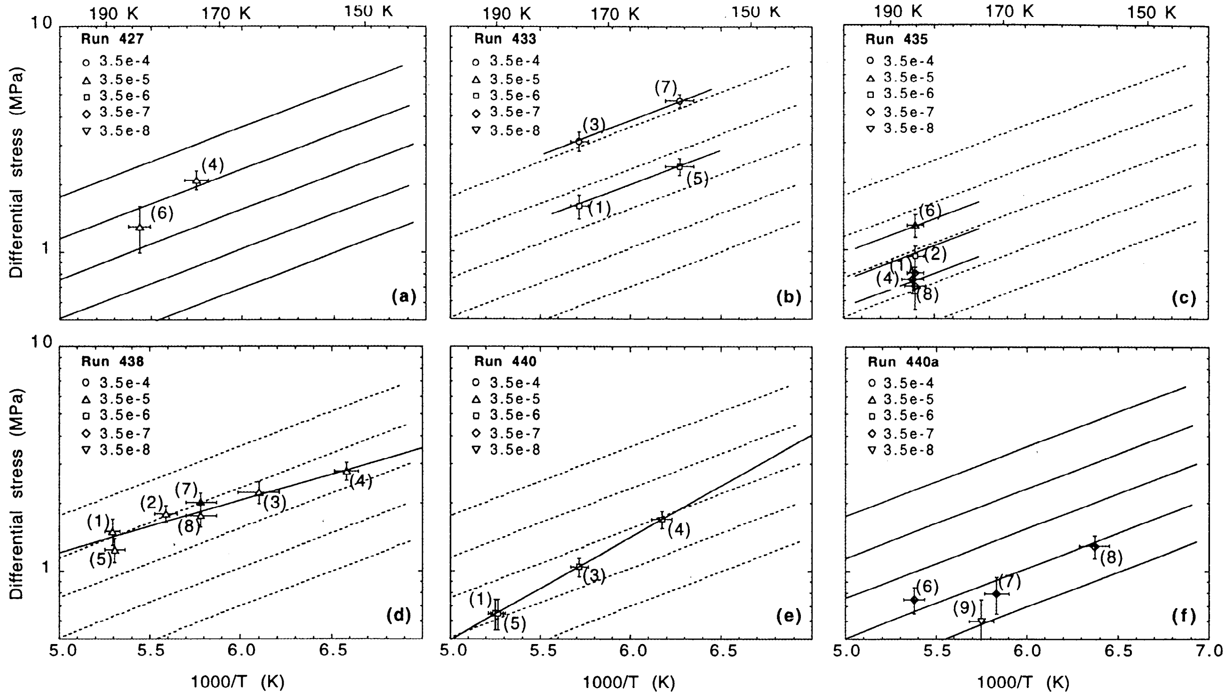

Figure 4. Flow data from Figure 2 broken out as individual runs. The five parallel lines of constant strain rate from Figure 2 are shown here as dashed where they are inconsistent with measurements for a particular run and as solid where they are consistent. Numbers in parentheses are run steps (Table 1).

manner. All of our experiments satisfy this requirement (Table 1). Consistent with these expectations, our triaxial tests on solid CO_2 do indicate somewhat higher strengths compared to those measured by *Clark and Mullin* [1976]. However, the main conclusion of Clark and Mullin stands that CO_2 is very much weaker than water ice, and where it exists, should flow easily over geologic time in the Martian polar caps. *Nye et al.* [2000] have performed preliminary modeling based on the results here and conclude that the Martian south polar cap probably is not composed primarily of CO_2 because the observed topography would relax too quickly by gravity-driven solid-state flow over the estimated age of the cap.

The high stress sensitivity of CO_2 is unusual but not unprecedented in geological materials near their melting point. The inconsistency between the n value calculated on the basis of all the runs (Figure 2) and on the basis of individual runs (Figure 4b and 4c), as well as the cause of sample-to-sample variability, requires further experimentation to resolve. Measurements of the strengths of solids bonded by weak van der Waals forces are sparse and not closely controlled [*Eluszkiewicz and Stevenson*, 1990], so it is difficult to determine whether the high n and strong variability are peculiar to CO_2 or are properties of this general class of materials.

Acknowledgments. This work was supported by NASA under order W-19,075. Work performed under the auspices of the U.S. Department of Energy by the Lawrence Livermore National Laboratory under contract W-7405-ENG-48. We thank D. L. Goldsby and D. L. Kohlstedt for their excellent reviews, which resulted in significant improvements to the figures and manuscript.

References

Clark, B. and R. Mullin, Martian glaciation and the flow of solid CO_2. *Icarus*, *27*, 215–228, 1976.

Durham, W. B., S. H. Kirby, and L. A. Stern, Creep of water ices at planetary conditions: a compilation, *J. Geophys. Res. (Planets)*, *102*, 16293-16302, 1997.

Eluszkiewicz, J. and D. J. Stevenson, Rheology of solid methane and nitrogen: applications to Triton, *Geophys. Res. Lett.*, *17*, 1753-1756, 1990.

Evans, B. and D. L. Kohlstedt, Rheology of Rocks, in *Rock Physics and Phase Relations, A Handbook of Physical Constants*, AGU Reference Shelf 3, 148–165, 1995.

Heard, H. C., Comparison of the flow properties of rock at crustal conditions, *Phil. Trans. R. Soc. London A.*, 283, 173-186, 1976.

Heard, H. C., W. B. Durham, C. O. Boro, and S. H. Kirby, A triaxial deformation apparatus for service at 77 ≤ T ≤ 273 K, in *The Brittle-Ductile Transition in Rocks, Geophysical Monograph 56*, ed. by A. G. Duba, W. B. Durham, J. W. Handin, and H. F. Wang, American Geophysical Union, Washington, D. C. 225-228, 1990.

Keiffer, H. H., Mars south polar spring and summer temperatures: A residual CO_2 frost, *J. Geophys. Res.*, *84*, 8263-8288, 1979.

Nye, J. F., W. B. Durham, P. M. Schenk and J. M. Moore, The stability of a South Polar Cap on Mars composed of carbon dioxide, *Icarus*, in press, 2000.

Paige, D. A. and K. D. Keegan, Thermal and albedo mapping of the polar regions of Mars using Viking thermal mapper observations 2. South polar region, *J. Geophys. Res.*, *99*, 25993 – 26013, 1994.

Paterson, M. S., Superplasticity in geological materials, in *Superplasticity in Metals, Ceramics, and Intermetallics, Mat. Res. Soc. Symp. Proc.*, *196*, ed. by M. J. Mayo, M. Kobayashi, and J. Wadsworth, Materials Research Society, pp. 303–312, 1990.

Thomas, P., S. Squyres, K. Herkenhoff, A. Howard, and B. Murray, Polar deposits of Mars, in *Mars*, ed. by H. H. Keiffer, B. M. Jakosky, C. W. Snyder, and M. S. Matthews, University of Arizona Press, Tucson, pp. 768-798, 1992.

Yamashita, Y. and M. Kato, Viscoelastic properties of polycrystalline solid methane and carbon dioxide, *Geophys. Res. Lett.*, *24*, 1327-1330, 1997.

W. B. Durham, University of California Lawrence Livermore National Laboratory, Livermore, CA 94550. (email: durham1@llnl.gov)

S. H. Kirby and L. A. Stern, United States Geological Survey, Menlo Park, CA 94025.

(Received June 4, 1999; revised August 27, 1999;
accepted September 21, 1999.)